

Coordinated development of the architecture of the primary shoot in bush rose

Sabine Demotes-Mainard, Gaëlle Gueritaine, Rachid Boumaza, Patrick Favre,
Vincent Guérin, Lydie Huché-Thélier, Bruno Andrieu

► **To cite this version:**

Sabine Demotes-Mainard, Gaëlle Gueritaine, Rachid Boumaza, Patrick Favre, Vincent Guérin, et al..
Coordinated development of the architecture of the primary shoot in bush rose. Third Symposium on
Plant Growth Modeling, Simulation Visualization and Applications, Nov 2009, Beijing (CH), China.
IEEE Computer Society, pp.214-221, 2009, <10.1109/PMA.2009.44>. <hal-00729988>

HAL Id: hal-00729988

<https://hal-agrocampus-ouest.archives-ouvertes.fr/hal-00729988>

Submitted on 5 Apr 2013

HAL is a multi-disciplinary open access archive for the deposit and dissemination of scientific research documents, whether they are published or not. The documents may come from teaching and research institutions in France or abroad, or from public or private research centers.

L'archive ouverte pluridisciplinaire **HAL**, est destinée au dépôt et à la diffusion de documents scientifiques de niveau recherche, publiés ou non, émanant des établissements d'enseignement et de recherche français ou étrangers, des laboratoires publics ou privés.

Coordinated Development of the Architecture of the Primary Shoot in Bush Rose

Demotes-Mainard S.^{1*}, Guéritaine G.¹, Boumaza R.², Favre P.¹, Guérin V.¹, Huché-Thélier L.¹,
Andrieu B.³

1 : INRA
UMR 462 SAGAH
IFR 149 Quasav

F-49071 Beaucouzé, France

* Corresponding author:

sabine.demotes@angers.inra.fr

2 : Agrocampus Ouest,
UMR 462 SAGAH
IFR 149 Quasav

F-49045 Angers, France

3 : INRA
UMR 1091 EGC,
F-78850 Thiverval-Grignon,
France

Abstract

The development of the architecture of ornamental bushes needs to be explicitly described because it defines both their visual appearance and their interface with the environment. The aim of this work was to describe the dynamics of organ development in the primary shoot of rose bushes and their coordination. Rosa hybrida L. 'Radrazz' was grown in a glasshouse in two seasons. Internodes and leaflets were measured frequently and elongation curves were fitted to a linear-plateau model. The number of leaflets per leaf displayed clear patterns of organization along the shoot. Allometric relationships linked all leaf dimensions to terminal leaflet length. The differences in internode length between successive phytomers resulted from differences in the extension rate and the duration of extension. Conversely, the differences in the terminal leaflet size resulted almost solely from differences in extension rate. Internodes and terminal leaflets extensions were closely coordinated. This work provides the basic elements for establishing a virtual plant model.

1. Introduction

The architecture of ornamental plants is important because it determines the organization of the plant and defines the properties of the plant-environment interface. It is also a determinant factor of the appearance of the plant, a key element of its commercial value. The modeling of ornamental plant architecture is therefore of great potential value. This study contributes to construct a model of the development of plant architecture in rosebushes, with a

view to improving our understanding of the plasticity of plant architecture and, subsequently, predicting the architectural response to different light conditions. Light modulates several processes of great importance for the quality of rosebushes. Bud burst is influenced by light quality and intensity [1] [2]. Flower development is enhanced by a high photon flux density [1] [3] and a high red:far red ratio [3], and stem length may be reduced [4] or increased [3] by increasing photon flux density. Light is perceived directly by buds [2] and shoot tips [5]. Estimations of the intensity and quality of light reaching specific rose organs is thus of great interest, but it is difficult to measure local light levels. The combination of a dynamic architectural plant model with a radiative transfer model simulating the distribution of light on plant organs could be used to analyze plant responses and to test hypotheses concerning these responses.

Models have already been developed to simulate the effect of growing conditions on the waves of flowering and the morphological quality of harvestable flowering shoots in cut-flower roses. In cut-flower roses the number of flowers produced is the most important variable. Only a few global variables are required to describe the visual quality of the flower, so models for these roses tend to describe architecture on the basis of stem length or diameter [6] [7], or morphological quality classes [8]. Structural descriptions have been refined further in more mechanistic models [9] [10], but only with a view to predicting the number of rose flowers more accurately. ROSEGRO [10], for example, is a photosynthesis-based model that predicts the number of flowering shoots and their average weight and length as a function of the climatic conditions in the greenhouse. ROSEGRO considers cohorts of phytomers, assuming that all phytomers appearing within a given time

interval have identical internode lengths and leaflet areas.

The development of rose architecture needs to be explicitly described as the commercial value of bush roses depends on plant shape in addition to flower production. The aim of this work was to acquire data on the dynamics of development and the final dimensions of the organs forming the primary shoot of the rosebush and to produce an organized description of these elements and of their relationships. These results present a general framework of primary shoot development that should be useful to develop an architectural model at the scale of the phytomer.

2. Materials and Methods

Roses (*Rosa hybrida*) of the ‘Radrazz’ cultivar, which grows as a bush, were grown in two experiments. One-node cuttings with 5- or 7-leaflet leaves were taken from cloned mother plants on 6 February and 25 April 2007, in experiments 1 and 2, respectively. Well-rooted cuttings were transferred to 1 liter pots on 7 March and 30 May 2007. Plants were grown in a glasshouse with one border row. Daylength was extended to 16 h using high-pressure sodium lamps. Mineral nutrition was provided by fertigation. Air temperature was measured above the canopy. Mean air temperature from bud emergence to sepal reflecting stage was 20.3 ± 4.0 and $21.7 \pm 3.4^\circ\text{C}$ in experiments 1 and 2, respectively. Thermal time was calculated from minimum and maximum daily values, with a base temperature of 2.1°C [11].

Results were obtained for the primary axis. Phytomers were numbered from the base to the top of the axis, and the peduncle was counted separately. Only phytomers with extended internodes, exceeding the threshold length of 1 mm, were counted. We use the definition of “phytomer” provided by Rutishauser [12], according to which a phytomer consists of an internode, the leaf at the top of the internode and its axillary bud.

Plants were monitored nondestructively three times per week in experiment 1 and five times per week in experiment 2. We assessed developmental stages: bud emergence, the presence of a visible flower bud, visible color of petals and sepal reflecting. The number of phytomers per shoot and the number of leaflets per leaf were counted. In experiment 1, we randomly selected three plants for dissection, three times per week, from 27 March to 3 May. The lengths and widths of the leaflets and of the leaf were measured, together with stipule length (Fig. 1), at four positions on the stem corresponding to the basal and apical 5-leaflet leaves, median 7-leaflet leaf and apical 3-leaflet leaf. The leaflets were named A to D, as described in Fig. 1. In experiment 2, we measured the lengths of the

terminal leaflet (A-leaflet) and internode with a ruler, from the day on which they appeared until they reached their final size, for each phytomer of 33 plants.

Another experiment carried out in the same compartment of the glasshouse at the same time as Exp. 2 showed that taking regular measurements of A-leaflet length reduced final internode length by 14%, but had no effect on A-leaflet length (Morel, personal communication), suggesting a possible effect of thigmomorphogenesis in Exp. 2.

3. Results

3.1. Distribution of number of leaflets per leaf along the axis

The number of phytomers per axis varied considerably within each experiment, from 6 to 12 in Exp. 1 and from 8 to 13 in Exp. 2, not including the peduncle. Axes with 11 phytomers were the most frequent in both experiments (28% and 37% of the plants in experiments 1 and 2, respectively).

The leaves had between 0 and 8 leaflets. Leaves with no leaflets were reduced to a stipule. This was the case at the base of the stem. For 11-phytomer plants, the most frequent number of leaflets per leaf increased progressively up the axis, from 0 at the base to 5 and then 7 at rank 7 (Fig. 2). From rank 8, the most frequent number of leaflets per leaf progressively decreased to 5 and then 3. At rank 11, 30% of the leaves had 1 leaflet. Most of the leaves (92.3%) had an odd number of leaflets or were reduced to a stipule. When present, leaves with an even number of leaflets were positioned so that their leaflet number was

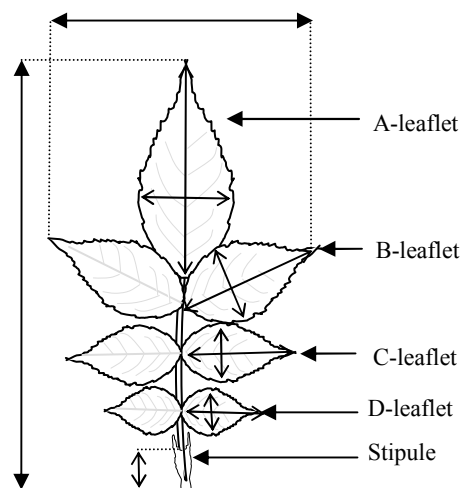


Fig. 1. Drawing of a 7-leaflet leaf of *Rosa hybrida*, cv ‘Radrazz’. Arrows show the measurements taken for leaf length and width, leaflet lengths and widths and stipule length. Leaflets are named A to D. In a 5-leaflet leaf there would be no D-leaflet.

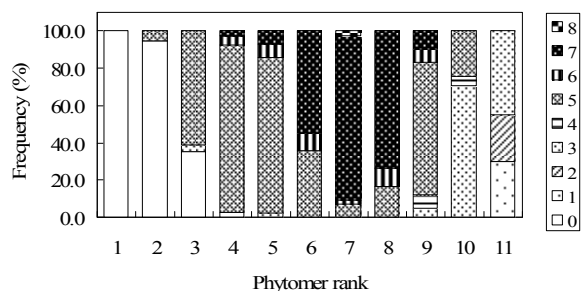


Fig. 2. Frequency of the number of leaflets per leaf for each phytomer rank on 11-phytomer (excluding the peduncle) primary axes, for 'Radrazz' cultivar roses grown in a glasshouse from March to May or from May to September 2007 (n=42 plants). Phytomer ranks are numbered acropetally.

intermediate between that of their neighbors, respecting the overall pattern of leaflet number increase and then decrease up the axis. No more than two classes of leaves (based on leaflet numbers) accounted for at least 10% of the leaves on any phytomer other than phytomer 11.

Similar trends were observed for all plants, regardless of the number of phytomers per axis (Fig. 3). The mean number of leaflets per leaf for the basal phytomers (ranks 2 and 3) was lower for axes with many phytomers than for axes with few phytomers, with the exception of nine-phytomer axes. Almost all

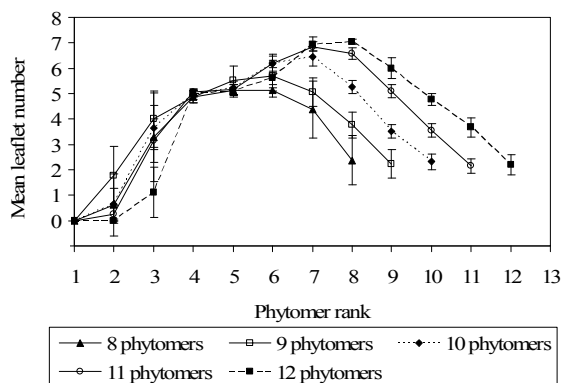


Fig. 3. Mean leaflet number per leaf at each phytomer rank for primary axes with 8 phytomers (n=8 plants), 9 phytomers (n=17 plants), 10 phytomers (n=31 plants), 11 phytomers (n=42 plants) and 12 phytomers (n=21 plants), excluding the peduncle, for roses of cultivar 'Radrazz' grown in a glasshouse from March to May or from May to September 2007. Phytomer ranks were numbered from the base to the top of the axes. Vertical bars indicate the 95% confidence interval.

the leaves on rank 4 had five leaflets, regardless of the number of phytomers per axis. The rank at which mean leaflet number peak was about 2/3 the total number of phytomers, starting from the base, for all curves. The maximum number of leaflets per leaf was strongly correlated with the number of phytomers per axis ($R_s=0.60$, $n=125$, $P<0.0001$), increasing from 5.1 in 8-phytomer axes to 7.0 in 12-phytomer axes, according to the proportion of 5- and 7-leaflet leaves. The mean number of leaflets of the apical leaf did not vary with the number of phytomers per axis.

3.2. Allometric relationships between all leaf dimensions and the length of the A-leaflet

Highly significant linear relationships linked the length of the A-leaflet with the lengths of the leaf, and of leaflets B, C and D (Tab. 1). Similarly, A-leaflet length was linearly related to the widths of the leaf, and of leaflets A, B, C and D. These relationships were weaker for the dimensions of the D-leaflets than for those of the other leaflets. Some of these relationships varied slightly with the number of leaflets per leaf. Stipule length was approximately constant from the time at which the stipule first became visible, at 1.01 ± 0.04 cm, for all leaf types. If required in modeling approaches, all regression constants can be forced to zero (R^2 between 0.96 and 0.99, data not shown), to reduce the number of parameters required to estimate leaf shape.

3.3. Extension of internodes and leaflets

The extension of internodes and A-leaflets (terminal leaflets) was studied on plants with 11 phytomers in experiment 2 (n=14 plants). For each plant, thermal time 0 was considered to be the time at which the peduncle was 1 cm long. This gave us a time origin related to the process of organ extension. The time at which the peduncle was 1 cm long was estimated by fitting a linear-plateau model to individual peduncle elongation curves against thermal time since bud emergence ($r^2=0.991$ to 0.999, with $n=12$ to 17, depending on the plant). The peduncle was studied because it gave a very good fit as it was longer than any other internode.

Fig. 4 shows a plot of A-leaflet and internode lengths divided by final length (normalized length) against thermal time, for phytomer 9 as an example. Final length varied between plants, from 6.1 to 7.3 cm for the A-leaflet at rank 9 and from 2.0 to 4.0 cm for internode 9. However, the time course of normalized length was similar for all plants, but with different time lags between plants. Thus, differences in final length between plants were due to differences in extension rates rather than differences in the duration of

Table 1. Linear regressions of A-leaflet length on the one hand with the lengths and widths of all leaflets and of the leaf on the other hand, for roses of cultivar ‘Radrazz’ grown in a glasshouse from March to May 2007. Regressions do not distinguish between leaves with different numbers of leaflets. All data are in centimeters. A-leaflet is the terminal leaflet, B, C and D leaflets are positioned in this order along the rachis, starting close to the terminal leaflet and progressing towards the stipule.

	Length (cm)				Width (cm)			
	<i>Slope ± se</i>	<i>Intercept ± se</i>	<i>R</i> ²	<i>df</i>	<i>Slope ± se</i>	<i>Intercept ± se</i>	<i>R</i> ²	<i>df</i>
Leaf	1.46±0.056**	2.07±0.34**	0.78	194	1.49±0.044**	-0.129±0.272 ns	0.87	174
A-leaflet					0.518±0.015**	-0.139±0.089 ns	0.86	193
B-leaflet	0.677±0.016**	0.463±0.094**	0.91	195	0.387±0.012**	0.0441±0.073 ns	0.84	192
C-leaflet	0.474±0.022**	0.768±0.135**	0.74	151	0.300±0.016**	0.186±0.092*	0.71	150
D-leaflet	0.330±0.043**	0.657±0.255*	0.56	47	0.186±0.030**	0.230±0.183 ns	0.45	46

** : significant at $P < 0.001$; * : significant at $P < 0.05$; ns: not significant

extension. This applied to all phytomers (data not shown for phytomers other than 9).

For each phytomer rank, all 11-phytomer plants were pooled together and curves of average A-leaflet and internode lengths against thermal time were fitted with a two-phase model, consisting of a linear phase followed by a plateau, as described in [13]. In cases in which final size varied significantly with leaflet number, only the data obtained for plants with the most frequent leaflet number were used. Internodes were systematically shorter and had shorter durations of extension and slower rates of extension than the A-leaflets of the same phytomer (Fig. 5). Elongation of A-leaflets and internodes, but not of the peduncle, was complete when the flower bud of the primary axis reached the visible color of petals (VCP) stage. A-leaflet extension began at almost the same time as extension of the internode from the same phytomer (Fig. 6). Furthermore, A-leaflet extension ended at about the same time as extension of the internode of the phytomer immediately above (Fig. 6).

Duration of the rapid extension phase, extension rate and final length, estimated from the fitted growth curves, are plotted against phytomer rank in Fig. 7. For A-leaflets, extension rate and final length differed considerably between phytomers (Fig. 7a), whereas the duration of the rapid extension phase was almost identical (Fig. 7b). Plots of the rate of A-leaflet extension during the linear phase and the final length of this leaflet plotted against phytomer rank followed a similar pattern (Fig. 7a): a sharp increase between ranks 3 and 5, and then a moderate increase to the top. Thus, differences in the final length of A-leaflets between phytomers resulted essentially from differences in extension rate rather than from differences in the duration of the extension phase.

Internode extension rate and final length followed similar patterns when these data were plotted against phytomer rank (Fig. 7c): an increase from rank 1 to 9

followed by a sharp decrease between ranks 9 and 11. The extension rate and final length of the peduncle were much greater than for any internode. The duration of the rapid extension phase increased from phytomers 1 to 5, was approximately stable for phytomers 6 to 9, increased moderately for phytomers 10 and 11 and sharply for the peduncle (Fig. 7d). Thus, differences in

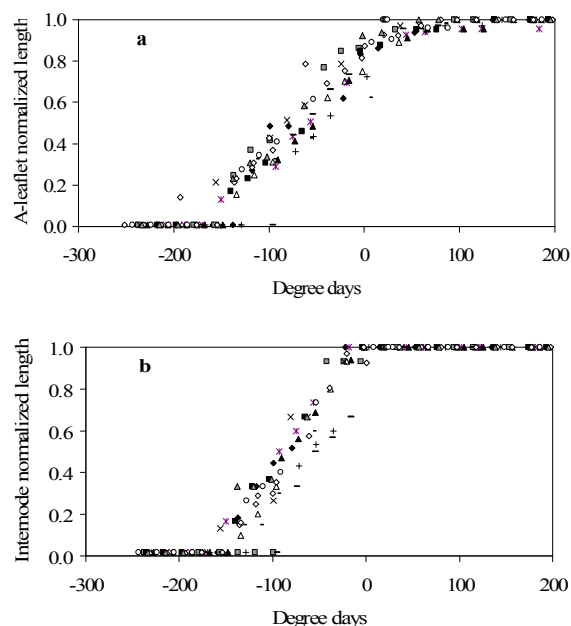


Fig. 4. Normalized terminal leaflet (A-leaflet) length (a) and internode length (b) for a phytomer of rank 9, plotted against thermal time, for roses of cultivar ‘Radrazz’ with 11 phytomer (excluding the peduncle) primary axes grown in a glasshouse from May to September 2007. Each symbol represents a plant. The thermal time origin corresponds to the time point at which the peduncle was 1 cm long.

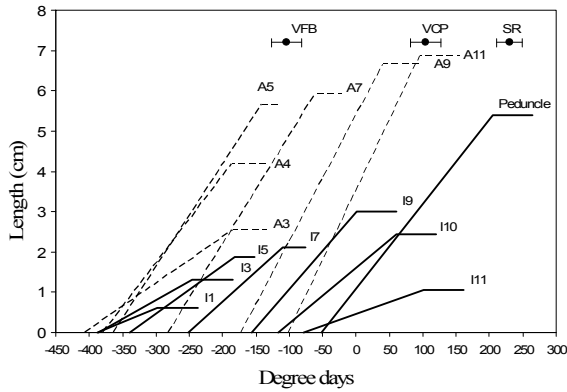


Fig. 5. Adjusted elongation curves for terminal leaflet (A-leaflet) length and internode length against thermal time, for roses of cultivar 'Radrazz' with 11 phytomer (excluding the peduncle) primary axes grown in a glasshouse from May to September 2007. Internodes of rank n are denoted "In", A-leaflets of rank n , An, and ranks are numbered acropetally. Leaflet lengths are plotted as dotted lines and internode lengths are plotted as continuous lines. Some leaflets and internodes are not shown, for the sake of clarity. Circles indicate the dates \pm standard deviation of the stages "visible flower bud" (VFB), "visible color of petals" (VCP) and "sepal reflecting" (SR). Thermal time origin corresponds to the time at which the peduncle was 1 cm long.

internode and peduncle final lengths between phytomers resulted from differences in the rate and duration of extension, except for the differences between phytomers 6 to 9, which were due solely to differences in extension rate.

4. Discussion, conclusion

The total number of phytomers on the main stem varied considerably between plants, despite the genetically identical nature of the plants studied (clones) and the selection of cuttings to limit variability. Similarly high levels of variability have been reported in other experiments [14] and may result from differences in leaf area between cuttings [7]. The variability of phytomer number leads to variability in the distribution of the different types of leaves along the axis and complicated architectural analysis. We therefore selected 11-phytomer plants for some aspects of this study.

The number of leaflets per leaf changed along the primary shoot in a well organized acropetal sequence: leaves were simple stipules at the base of the axis, with the number of leaflets gradually increasing to 5 or 7 in

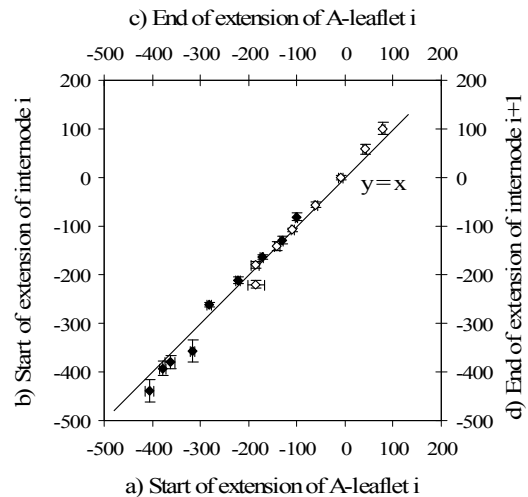


Fig. 6. Thermal time at the start of the rapid extension phase for an A-leaflet of rank i (a), plotted against thermal time at the start of the rapid extension phase for an internode of rank i (b) (plain symbols). Thermal time at the end of the rapid extension phase for an A-leaflet of rank i (c) plotted against thermal time at the end of the rapid extension phase for an internode of rank $i+1$ (d) (open symbols), for roses of cultivar 'Radrazz' with 11 phytomer (excluding the peduncle) primary axes grown in a glasshouse from May to September 2007; $i=3$ to 10. The thermal time origin is the time point at which the peduncle was 1 cm long. The A-leaflet is the terminal leaflet. Vertical and horizontal bars indicate the standard deviation.

the median zone, and then decreasing to 3, 2 or 1 at the top of the axis. This general pattern is common to many species and rose varieties, but with some variability [15]. In a dynamic model, it is important to describe this pattern for the simulation of leaf area. In our experiments, knowing the final number of phytomers, the mean number of leaflets per leaf could be described with a small number of parameters.

The compound nature of rose leaves and variability in the number of leaflets per leaf made it necessary to establish allometric relationships for individual leaf components, facilitating description of the leaf with only a small number of parameters. We were able to estimate the shape of a leaf at any stage of growth, from the number of leaflets and the length of the A-leaflet, using a single set of parameters.

Studies on various species have reported that extension of leaves and internodes starts with an exponential phase, (e.g. [16] [17] [18] [19]). This is very likely the case in rose and was actually suggested in some of our data (not shown). However, the length

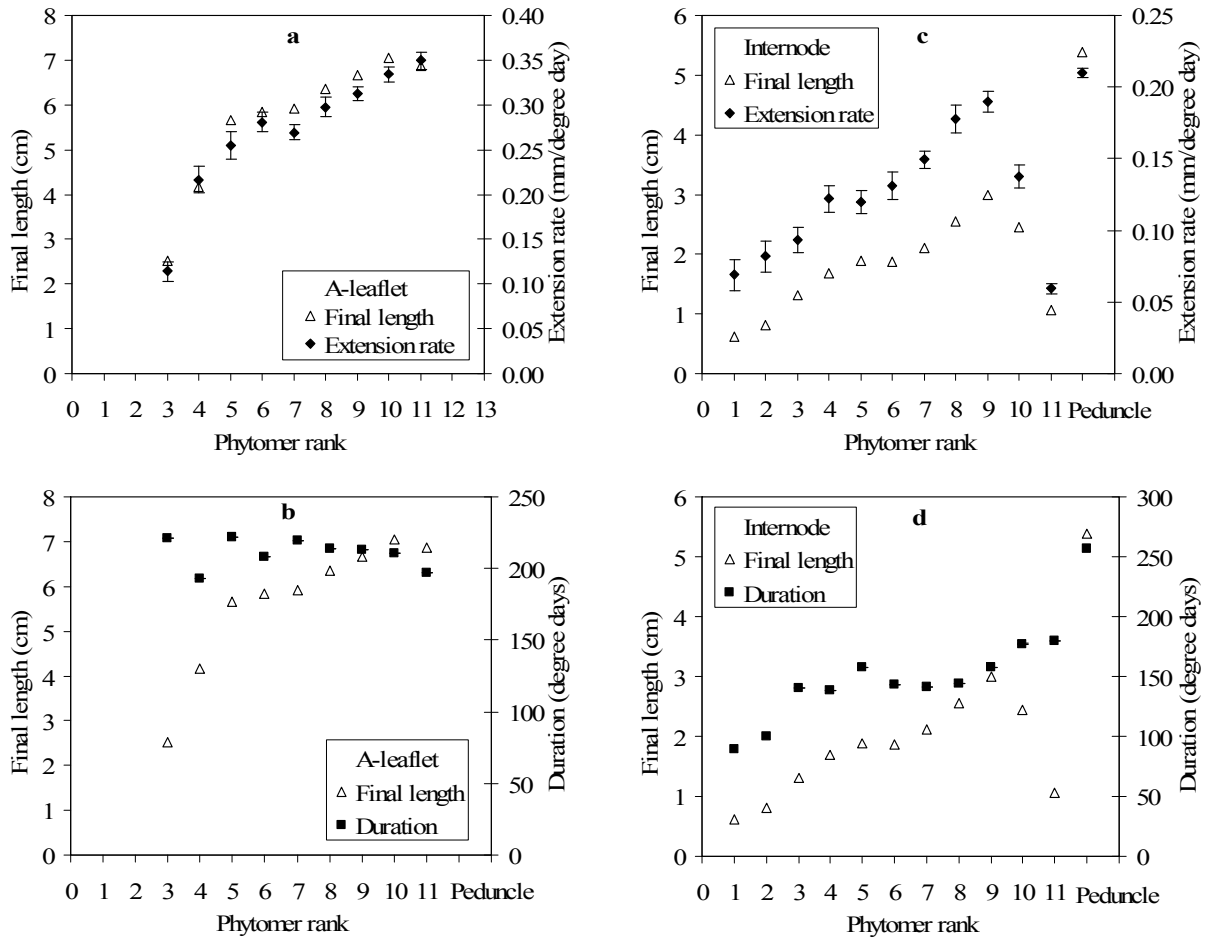


Fig. 7. Final length and extension rate of the A-leaflet (a) and internode (c) against phytomer rank. Final length and duration of the rapid extension phase of the A-leaflet (b) and internode (d) against phytomer rank. Data obtained on roses of cultivar 'Radrass' with 11 phytomer (excluding the peduncle) primary axes grown in a glasshouse from May to September 2007. The A-leaflet is the terminal leaflet. Extension rate, duration of the rapid extension phase and final length are calculated from adjusted growth curves, using a linear-plateau model. The rate and duration of extension were estimated as the slope and duration of the linear phase, respectively. The plateau value was used as an estimate of final length. Vertical bars indicate the standard deviation.

reached at the end of the exponential phase is short, and given the time interval between successive measurements in our experiment, it was possible to identify such exponential phase only for a few phytomers. We therefore used a linear-plateau model that allowed to keep a consistent set of parameters to describe the whole series of phytomers [13].

Differences in final A-leaflet length between phytomer ranks were linked to differences in extension rates, with the duration of extension similar for all phytomer ranks. Similar results have been reported for wheat [16], but the duration of expansion has been found to differ between phytomers in other species, such as sunflower [17] and maize [18]. Internodes

behaved differently, as the differences in final length between phytomers resulted from differences in both the rate and duration of extension for internodes 1 to 5 and 10 to peduncle, and differences in extension rate only for internodes 6 to 9. A difference in behavior between lower and upper internodes was also observed for maize [19].

Differences between plants in the final lengths of both the A-leaflet and the internode for phytomer 9 were linked to differences in the rate of extension, in the absence of a difference in the duration of extension. This was demonstrated for phytomer 9 but appeared to be a general feature in our experiment. This stability of the duration of extension should be evaluated over a

range of growth conditions. If confirmed, it would greatly simplify model development, as we would then need to take into account only variations of the rate of extension, without needing to consider variations of the duration of extension.

Models of the dynamics of architecture development in roses should be parameterized using the series of 2-phase models of internode and terminal leaflet growth curves against phytomer rank. Coordination between the extension phases of the A-leaflets and internodes may optimize parameterization of the dates on which extension starts and stops for successive A-leaflets and internodes along the axis, thereby simplifying the model. The stability of the coordination of A-leaflet and internode extension should be assessed over a range of growing conditions and genotypes.

As the visual appearance of a rosebush depends on the number and rank of lateral shoots, we will also study the lateral shoots: at what phytomer rank and when do buds burst? To what extent is the pattern described here modified in lateral shoots?

In conclusion, this work provides a global framework for the development of plant architecture for the primary shoots of rosebushes. It constitutes a solid basis for the establishment of a virtual plant model. This framework has two main types of application. Firstly, it defines a grid for analyzing the response of rose phenotypic development to environment, genotype and genotype \times environment interactions. Secondly, the implementation of the virtual plant model and its coupling with a radiative transfer model [20] should make it possible to simulate light distribution over plant organs and to test hypotheses concerning plant responses.

5. Acknowledgment

The authors thank O. Douillet and S. Delépine (INRA, UMR SAGAH) for assistance with the experimental measurements, G. Guillemain (INRA, UMR SAGAH) for maintaining growth conditions and M. Laffaire (Agrocampus-Ouest, UMR SAGAH) for plant multiplication. J. Sappa (scientific translator, Alex Edelman & Associates) reviewed the paper for English usage. This work was supported by Angers Loire Métropole, through a postdoctoral grant.

6. References

[1] Y. Mor, and A. H. Halevy, "Dual effect of light on flowering and sprouting of rose shoots", *Physiol. Planta.*, 1984, 61, 119-124.
 [2] T. Girault, V. Bergougnoux, D. Combes, J.D. Viemont and N. Leduc, "Light controls shoot meristem organogenic activity and leaf primordia growth during bud burst in *Rosa* sp." *Plant Cell Env.*, 2008, 31, 1534-1544.

[3] F.M. Maas and E. J. Bakx, "Effects of light on growth and flowering of *Rosa hybrida* Mercedes", *J. Amer. Soc. Hort. Sci.*, 1995, 120, 571-576.
 [4] N. Bredmose, "Growth, flowering, and post-harvest performance of single-stemmed rose (*Rosa hybrida* L.) plants in response to light quantum intergral and plant population density", *J. Amer. Soc. Hort. Sci.*, 1998, 123, 569-576.
 [5] Y. Mor, and A. H. Halevy, "Characterization of the light reaction in promoting the mobilizing ability of rose shoot tips", *Plant Physiol.*, 1980, 66, 996-1000.
 [6] D.A. Hopper, P.A. Hammer and J.R. Wilson, "A simulation model for *Rosa hybrida* growth response to constant irradiance and day and night temperatures", *J. Amer. Soc. Hort. Sci.*, 1994, 119, 903-914.
 [7] J.M. Costa and E. Heuvelink, "Modelling growth of the primary shoot of rose", *Acta Hort.* 2004, 654, 279-285
 [8] A. Morisot, "PP.Rose: an empirical model to predict the potential yield of cut roses", *Acta Hort.*, 1996, 424, 87-93.
 [9] J.H. Lieth and C. Passian, "A simulation model for the growth and development of flowering rose shoots", *Scientia Hort.*, 1991, 46, 109-128.
 [10] E.E. Dayan, E. Presnov and M. Fuchs, "Prediction and calculation of morphological characteristics and distribution of assimilates in the ROSGRO model", *Mathematics and Computers in Simulation*, 2004, 65, 101-116.
 [11] C. Massot, "Détermination de la température de base et des unités thermiques accumulées pour différentes phénophases des rosiers *Rosa x hybrida* 'Knock Out et *Rosa wichurana*", Master report, Université d'Angers, France, 2007, 28p., unpublished.
 [12] R. Rutishauser, "Developmental patterns of leaves in Podostemaceae compared with more typical flowering plants: saltational evolution and fuzzy morphology", *Can. J. Bot.*, 1994, 73, 1305-1317.
 [13] J. Hillier, D. Makowski and B. Andrieu, "Maximum likelihood inference and bootstrap methods for plant organ growth via multi-phase kinetic models and their application to maize", *Annals Bot.*, 2005, 96, 137-148.
 [14] Ph. Morel, G. Galopin and N. Donès, "Using architectural analysis to compare the shape of two hybrid tea rose genotypes", *Scientia Hort.*, 2009, 120, 391-398.
 [15] M. Le Bris, A. Champeroux, P. Bearez and M.T. Le Page-Degivry, "Basipetal gradient of axillary bud inhibition along a rose (*Rosa hybrida* L.) stem: Growth potential of primary buds and their two most basal secondary buds as affected by position and age", *Annals Bot.*, 1998, 81, 301-309.
 [16] C. Fournier, J. Durand, S. Ljutovac, R. Schäufele, F. Gastal and B. Andrieu, "A functional-structural model of elongation of the grass leaf and its relationships with the phyllochron", *New Phytol.*, 2005, 166, 881-894.
 [17] G.A.A Dosio, H. Rey, J. Lecoeur, N.G. Izquierdo, L.A.N. Aguirrezzabal, F. Tardieu and O. Turc, "A whole-plant analysis of the dynamics of expansion of individual leaves of two sunflower hybrids", *J. Exp. Bot.*, 2003, 54, 2541-2552.
 [18] B. Andrieu, J. Hillier, C. Birch, "Onset of sheath extension and duration of lamina extension are major determinants of the response of maize lamina length to plant density", *Annals Bot.*, 2006, 98, 1005-16.
 [19] C. Fournier and B. Andrieu, "Dynamics of the elongation of internodes in maize (*Zea mays* L.): analysis of

phases of elongation and their relationships to phytomer development", *Annals Bot.*, 2000, 86, 551-563.

[20] M. Chelle and B. Andrieu, "Modelling the light environment of virtual crop canopies". In *Functional-Structural Plant Modelling in Crop Production*, ed. J. Vos, L. Marcelis, P. DeVisser, P. Struik, J. Evers, Springer, Wageningen, The Netherlands, 2007, 75-89.